

## The Structural Basis for Pseudoreversion of the H95N Lesion by the Secondary S96P Mutation in Triosephosphate Isomerase<sup>†,‡</sup>

Elizabeth A. Komives,<sup>\*,§</sup> Julie C. Loughheed,<sup>§</sup> Zhidong Zhang,<sup>||</sup> Shigetoshi Sugio,<sup>⊥</sup> Narendra Narayana,<sup>§</sup> Nguyen H. Xuong,<sup>§</sup> Gregory A. Petsko,<sup>⊥</sup> and Dagmar Ringe<sup>⊥</sup>

Department of Chemistry and Biochemistry, University of California, San Diego, La Jolla, California 92093-0601, Department of Biology, Massachusetts Institute of Technology, Cambridge, Massachusetts 02139, and Departments of Biochemistry and Chemistry, Rosensteel Basic Medical Sciences Research Center, Brandeis University, Waltham, Massachusetts 02254-9110

Received June 27, 1996; Revised Manuscript Received September 20, 1996<sup>®</sup>

**ABSTRACT:** The structural basis for the 3000-fold decrease in catalytic efficiency of the H95N mutant chicken triosephosphate isomerase and the 60-fold regain of catalytic efficiency in the double mutant, H95N·S96P, have been analyzed. The results from a combination of X-ray crystallography and Fourier transform infrared spectroscopy experiments indicate that the predominant defect in the H95N mutant isomerase appears to be its inability to bind the substrate in a coplanar, *cis* conformation. The structures of each mutant isomerase were determined from X-ray crystallography of the complex of phosphoglycolohydroxamate (PGH), an intermediate analog, with the isomerase, and each was solved to a resolution of 1.9 Å. The PGH appeared to be in two different conformations in which the enediol-mimicking atoms, O2-N2-C1-O1, of the PGH were not coplanar. No density was observed that would correspond to the coplanar conformation. Two bands are observed for the dihydroxyacetone phosphate carbonyl in the H95N mutant FTIR spectrum, and these can be explained if the O1 of DHAP, like the O1 of PGH in the crystal structure, is in two different positions. Two ordered water molecules are located between O1 of PGH and Nδ of N95. Comparison of the structure of the pseudorevertant, H95N·S96P with that for the H95N single mutant, shows that S96P mutation causes the double mutant to regain the ability to bind PGH predominantly in the coplanar, *cis* conformation. Electron density for a single ordered water molecule bridging the N95 amide side chain and the O2 of PGH is observed, but the density was weak, perhaps indicating that the water molecule is somewhat disordered. Whether or not a water molecule is hydrogen bonded to O2 of PGH may explain the two carbonyl stretching frequencies observed for the GAP carbonyl. Together, the crystal structures and the FTIR data allow a complete explanation of the catalytic properties of these two mutant isomerases.

Triosephosphate isomerase (TIM) catalyzes the interconversion of dihydroxyacetone phosphate (DHAP) and glyceraldehyde 3-phosphate (GAP) (Figure 1). The reaction rate is limited by the rate of diffusion of substrate onto and off of the isomerase surface (Blacklow et al., 1988), and thus TIM is said to have evolved to catalytic perfection (Albery & Knowles, 1976; Knowles & Albery, 1977). Several experimental techniques have been applied to TIM in order to determine its catalytic mechanism and the way in which the structure of the enzyme supports the mechanism. We utilized two such techniques in the work presented here, both of which have been applied previously to wild-type TIM as well as several mutants. X-ray crystallography of the complex of TIM with phosphoglycolohydroxamate (PGH) is thought to give the best approximation of the structure of the enzyme in its catalytically competent form (Davenport et al., 1991; Zhang et al., 1994). In particular, the two

oxygens of PGH (O1 and O2) are thought to occupy similar sites as the carbonyl of DHAP (O1) and the carbonyl of GAP (O2) (Figure 1A). Fourier transform infrared spectroscopy (FTIR) has allowed observation of the carbonyl groups of the substrates when bound to the enzyme and has proven useful in determining the degree to which the enzyme polarizes the substrate carbonyl groups toward the transition state of the reaction (Belasco & Knowles, 1980; Komives et al., 1991). Much mechanistic information has been gained from attempts to correlate the observed carbonyl stretching frequencies for the carbonyl group of DHAP and GAP while bound to the enzyme with structural information from crystallographic analysis of the enzyme complexed with PGH (Komives et al., 1995).

Triosephosphate isomerase has several active site residues responsible for catalysis including E165, the catalytic base, which is positioned above the substrate in the active site, H95, the residue that appears to be responsible for shuttling protons between the two oxygens of the enediolate intermediates in the reaction, and K13, which is responsible for creating a positive environment in the active site so that the phosphodianion substrate can bind (Figure 2) (Zhang et al., 1994). S96 is also present in the active site and the side chain of this residue is in a different position in the substrate-free isomerase structure compared to the isomerase–PGH complex (Figure 2 and 3) (Lolis et al., 1990). In the

<sup>†</sup> Supported in part by a grant from Lucille P. Markey Charitable Trust and by a grant from the National Institutes of Health (GM-26788) to D. Ringe.

<sup>‡</sup> PDB Files: 1tpu = H95N TIM; 1tpv = H95N·S96P TIM; 1tph = wild-type TIM.

<sup>\*</sup> Author to whom correspondence should be addressed.

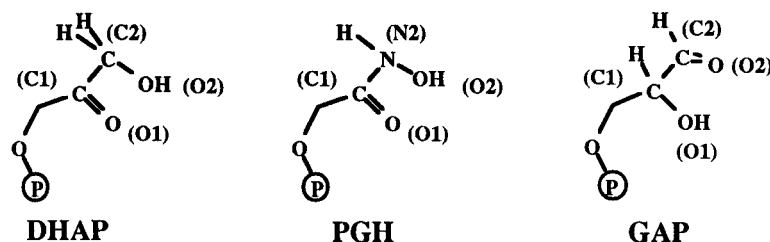
<sup>§</sup> UCSD.

<sup>||</sup> MIT.

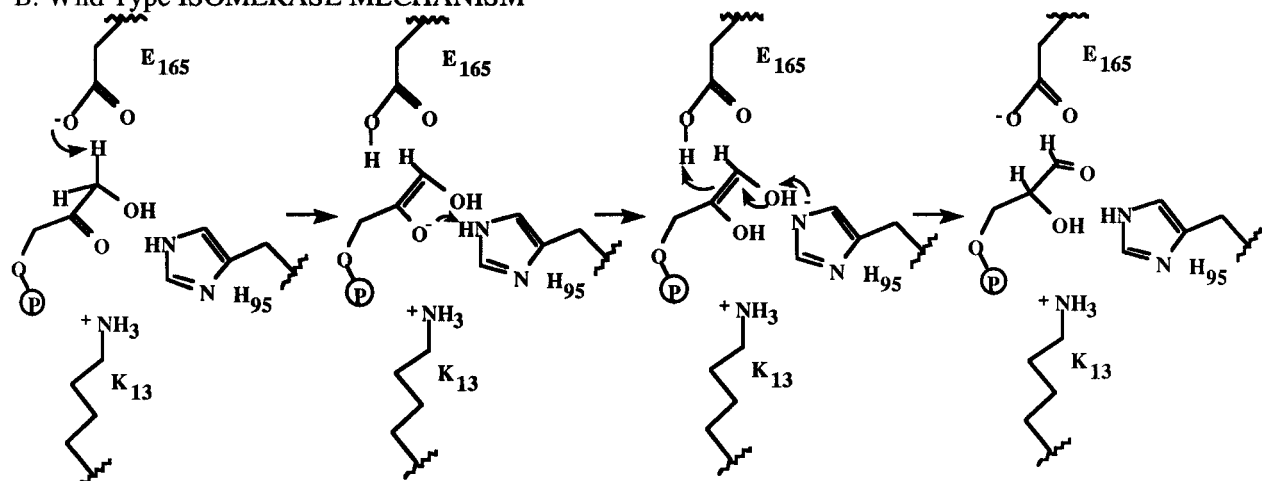
<sup>⊥</sup> Brandeis University.

<sup>®</sup> Abstract published in *Advance ACS Abstracts*, November 1, 1996.

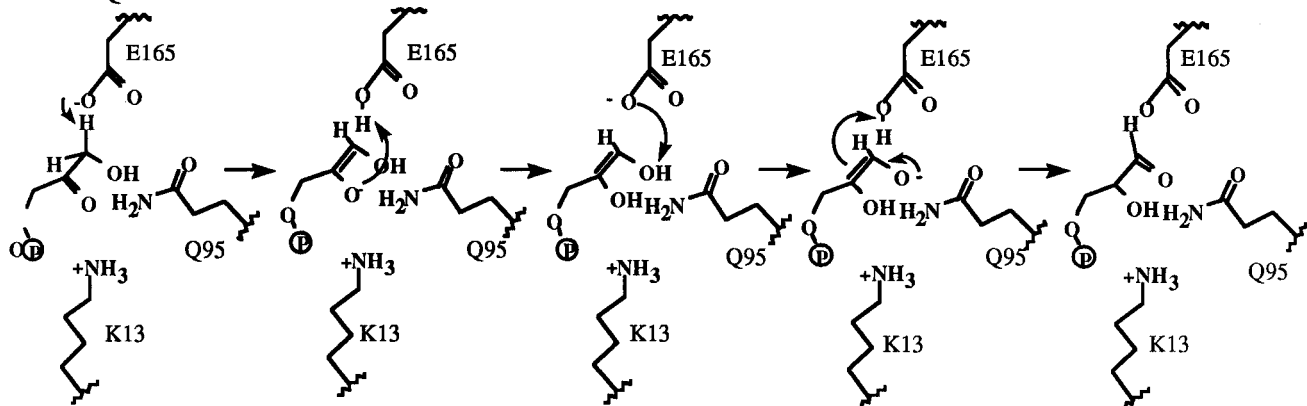
## A. Atom Designations for DHAP, PGH, and GAP



## B. Wild Type ISOMERASE MECHANISM



## C. H95Q Mutant ISOMERASE MECHANISM



## D. MECHANISM of Methylglyoxal Production

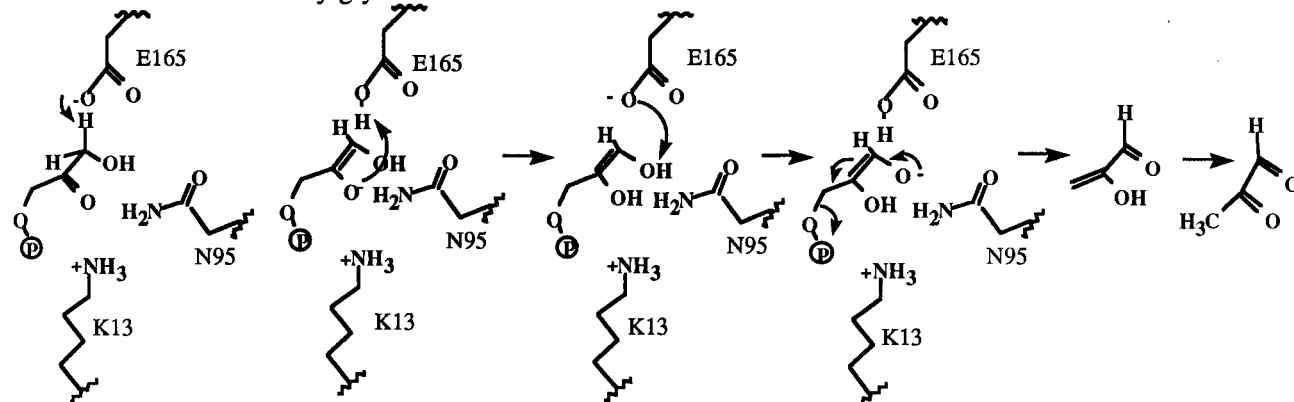


FIGURE 1: A. Schematic of DHAP, phosphoglycolohydroxamate, and GAP in the coplanar *cis* conformation found in the active site of the wild-type isomerase. The atoms of each molecule are numbered as they are cited in the text. B. Mechanism of the conversion of dihydroxyacetone phosphate to D-glyceraldehyde 3-phosphate by triosephosphate isomerase. C. Alternate mechanism of conversion of dihydroxyacetone phosphate to D-glyceraldehyde 3-phosphate by the H95Q mutant of triosephosphate isomerase. D. Mechanism of the conversion of dihydroxyacetone phosphate to methylglyoxal, a side reaction in the conversion of dihydroxyacetone phosphate to D-glyceraldehyde 3-phosphate by some mutants of triosephosphate isomerase.

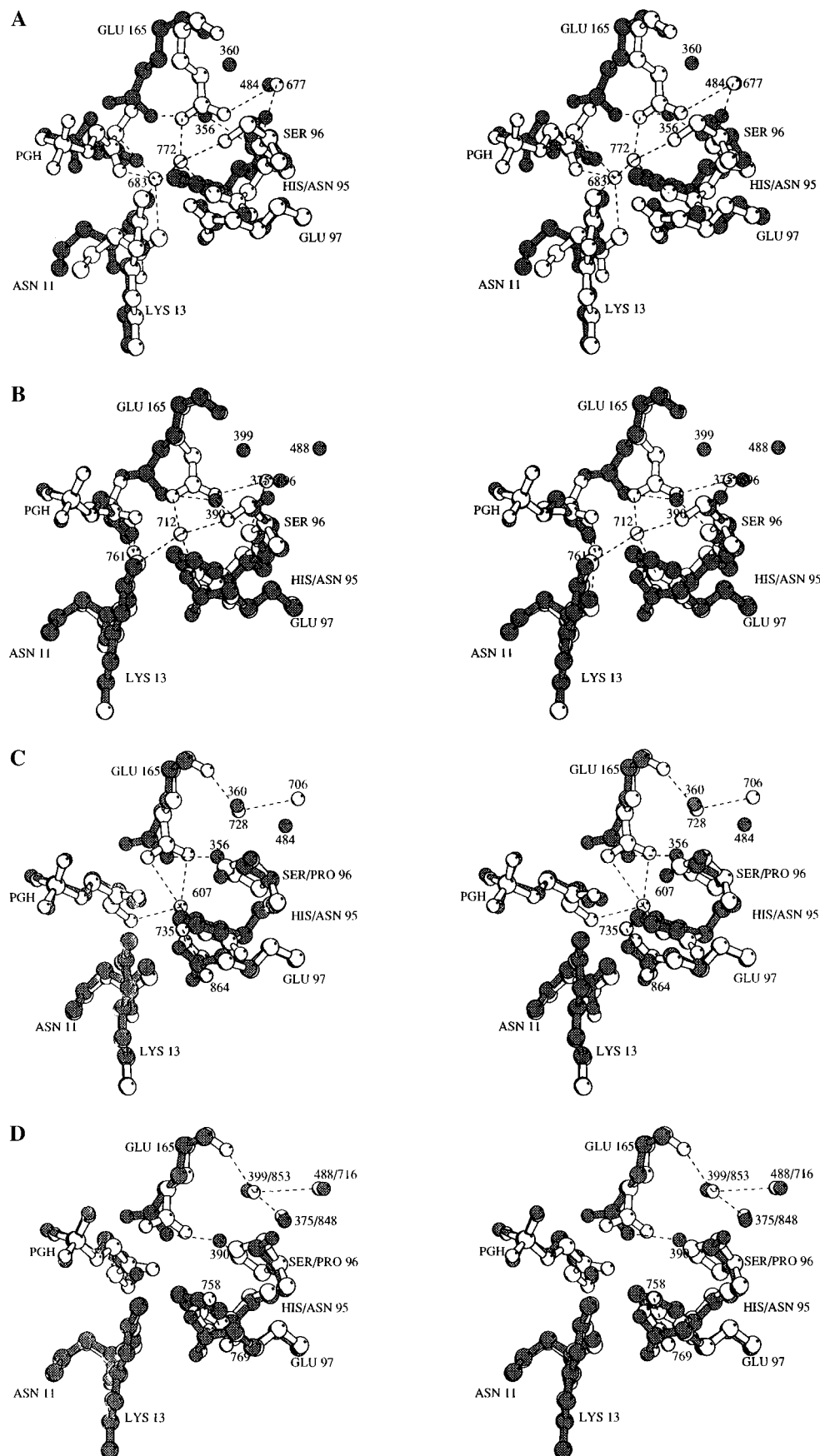


FIGURE 2: (A, B) Stereoview of the active sites after backbone superposition of subunit A or subunit B of the single mutant H95N isomerase (white) with the wild-type isomerase (grey). (C, D) Stereoview of the active sites after backbone superposition of subunit A or subunit B of the H95N-S96P double mutant isomerase (white) with the wild-type isomerase (grey). All structures were determined with the intermediate analog, PGH bound at the active site. Residues that may be involved in hydrogen bond interactions and were closer than 3.8 Å are connected by dashed lines.

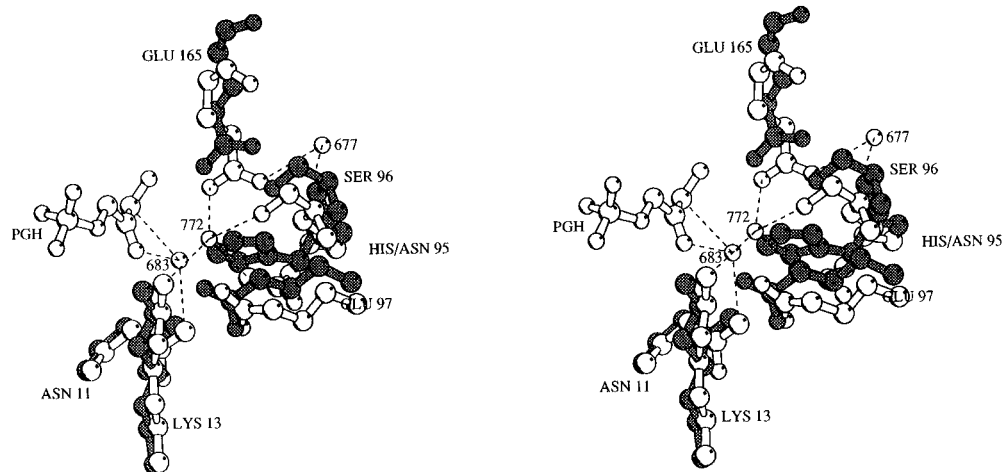


FIGURE 3: Stereoview of the active sites after backbone superposition of each subunit of the single mutant H95N isomerase with one subunit of the wild-type isomerase. The structure of the mutant was determined with the intermediate analog, PGH bound at the active site, the structure of the wild-type isomerase is the substrate-free form. Residues that may be involved in hydrogen bond interactions and were closer than 3.8 Å are connected by dashed lines.

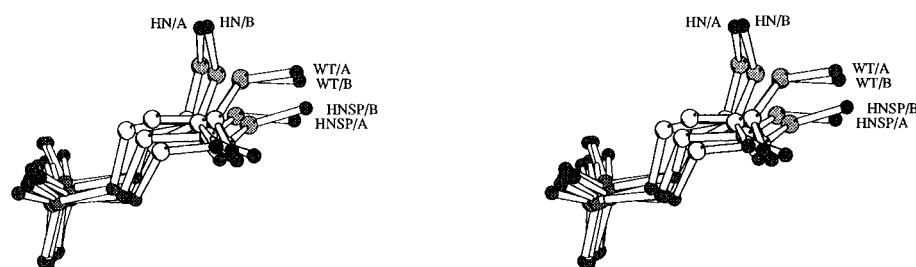


FIGURE 4: Stereoview of the PGH substrate analog molecules present at the active sites of each subunit of the isomerases. To obtain the best comparison of the orientations of the substrate analogs, the backbones of each isomerase were superposed. The PGH molecules are from each subunit of the single mutant H95N isomerase, each subunit of the double mutant H95N·S96P isomerase, and both subunits of the wild-type isomerase.

substrate-free form of the enzyme, the side chain of E165 is swung away from the substrate and the carboxyl group is within hydrogen-bonding distance of the hydroxyl group of S96. In the substrate-bound form, one carboxylate oxygen of E165 forms the apex of a distorted square pyramid, the base of which is formed by the O2-N2-C1-O1 plane of the substrate analog, PGH (Figure 4). The carboxyl group is no longer hydrogen bonded to the serine but is instead perfectly positioned to carry out proton transfers between C2 of DHAP and C1 of GAP (Figures 1B and 3).

The structure of the wild-type isomerase bound to the intermediate analog, PGH shows that H95 is perfectly positioned between the two oxygens of the substrate suggesting that this residue is responsible for shuttling protons between the two oxygens during the isomerization reaction (Zhang et al., 1994). Exchange-conversion experiments carried out on the wild-type isomerase showed that approximately 4% of tritium label at C1 of DHAP was transferred to C2 of the product, GAP. Mutation of H95 to glutamine in the yeast isomerase resulted in an isomerase enzyme in which the proton transfer mechanism had been subtly altered so that no tritium transfer was observed (Nickbarg et al., 1988). The H95Q mutant showed no transfer of tritium label from C2 of DHAP to C1 of GAP, and a mechanism in which the catalytic base (E165) carries out all the proton transfer steps was proposed (Figure 1C). In this mechanism, E165 abstracts the tritium from a non-solvent-exchangeable position, but transfers it to the enediolate oxygen, a solvent-exchangeable position. Therefore, all of the tritium washes out, and none is observed to be

directly transferred to C1 of GAP. This mechanism is also consistent with the crystal structure of the H95Q mutant isomerase in which E165 is repositioned so as to be within proton transfer distance of both the substrate carbons and oxygens (Komives et al., 1991). Additionally, FTIR experiments designed to observe the carbonyl groups of the bound substrate molecules in the yeast H95Q mutant isomerase showed the carbonyl groups of both DHAP and GAP at  $1740\text{ cm}^{-1}$ , nearly the same as DHAP and GAP free in solution. In contrast, the DHAP carbonyl group absorbs at  $1715\text{ cm}^{-1}$  when bound to the wild-type isomerase indicating substantial polarization of the substrate carbonyl group (Table 1). Unlike the H95Q mutant isomerase, both the single (H95N) and double (H95N·S96P) mutants did show transfer of tritium from C2 of DHAP to C1 of GAP suggesting they did not follow the altered mechanism seen for the H95Q mutant (Blacklow & Knowles, 1990). These results could be explained if a water molecule fit into the active site only when H95 was substituted with N and not with Q. In the H95N mutant, the water molecule could carry out the proton transfer steps ordinarily performed by H95.

In all crystal structures determined to date, the intermediate analog, phosphoglycolohydroxamate, PGH, is bound in a coplanar, *cis* conformation in which the phosphate ester is in the same plane as the carbonyl group and the hydroxamate hydroxyl group. Thus, the enediol resulting from deprotonation of DHAP or GAP, and therefore the atoms O1-C1-C2-O2 are coplanar, and the phosphate ester is in the same plane formed from these atoms (Figure 1A). Stereoelectronic considerations suggest that elimination (Figure 1D) is

Table 1: Infrared Data and Kinetic Constants for the H95N and H95N•S96P Mutant Isomerases Compared to Those of the H95Q and Wild-Type Isomerase

	H95N TIM	H95N•S96P TIM	H95Q TIM	wild-type TIM
Carbonyl Stretching Frequencies (in $\text{cm}^{-1}$ ) <sup>a</sup>				
DHAP	1725, 1735	1717	1745	1715, 1730
GAP	1745	1745, 1737	1745	NO <sup>b</sup>
Kinetic Constants <sup>c</sup>				
$K_{\text{mDHAP}}$ (mM)	0.59	0.40	2.5	0.65
$k_{\text{catDHAP}}$ ( $\text{s}^{-1}$ )	0.16	6.8	1.2	600
$k_{\text{cat}}/K_{\text{mDHAP}}$ ( $\text{M}^{-1}\cdot\text{s}^{-1}$ )	0.27	17	0.48	923
$n$ -fold decrease from wild type ( $n$ )	3400	54	1920	
$K_{\text{mGAP}}$ (mM)	0.08	0.08	0.43	0.42
$k_{\text{catGAP}}$ ( $\text{s}^{-1}$ )	0.46	29	4.4	8300
$k_{\text{cat}}/K_{\text{mGAP}}$ ( $\text{M}^{-1}\cdot\text{s}^{-1}$ )	5.75	363	10.2	19760
$n$ -fold decrease from wild type ( $n$ )	3400	54	1930	

<sup>a</sup> The values for the wild-type isomerase were reported previously (Belasco & Knowles, 1980). <sup>b</sup> NO, not observed. <sup>c</sup> The kinetic constants for the H95N and H95N•S96P were reported previously (Blacklow & Knowles, 1990).

minimized when orbital overlap between the enediolate  $\pi$  system and the C—O bond to the phosphate is avoided (Deslongchamps et al., 1972; Kirby, 1983). If orbital overlap occurs, as it does when the enediolate intermediate is generated free in solution, rapid elimination of phosphate and formation of methylglyoxal occurs (Richard, 1984). Two site-directed mutants that have been studied previously have been shown to form methylglyoxal as a by-product during turnover. The  $\Delta$ loop mutant, in which four residues of the flexible loop that covers the active site were deleted, formed three molecules of methylglyoxal for each turnover to DHAP from GAP, suggesting that the loop is required to sequester the intermediate from solvent water molecules (Pompliano et al., 1990). The H95N mutant formed three molecules of methylglyoxal for every ten turnovers to DHAP or GAP (Blacklow & Knowles, 1990). The cause of the production of methylglyoxal by the H95N mutant has not been determined, but at least three possibilities exist. First, the loop may not close properly letting water molecules into the active site which could catalyze the phosphate elimination. Second, the enzyme may bind the substrate in a noncoplanar conformation resulting in orbital overlap within the enediolate intermediate which would be expected to cause elimination of phosphate. Molecular dynamics calculations by Daggett and Kollman (1990) suggested that mutation of H95N in triosephosphate isomerase may result in distortion of the bound substrate toward a conformation in which the O2-C2-C1-O1 of the substrate were no longer coplanar; however, it should be noted that for elimination to be favored, the phosphate ester must be nonplanar with respect to the plane of the enediolate. Third, the enzyme may only slowly convert the enediolate to product, in which case a small amount of elimination may occur even from the unfavored planar conformation of the enediolate intermediate.

Attempts to restore activity in catalytically damaged mutants, E165D and H95N by random mutagenesis, gave the surprising result that the same second site alteration of serine 96 to proline (S96P) improved the catalytic efficiency of both the E165D mutant isomerase (by 20-fold) and the H95N mutant isomerase (by 60-fold) (Table 1) (Hermes et al., 1990; Blacklow & Knowles, 1990). Structural studies

on the E165D and E165D•S96P mutants suggested that the increased activity of the double mutant caused alterations of ordered water molecules within the active site of the isomerase which resulted in ground state stabilization of the first intermediate in the pathway, the enediolate (Komives et al., 1995).

We here report a series of X-ray crystallography and FTIR studies aimed at determining the structural basis of the defect in the H95N mutant isomerase and the improvement in catalytic activity caused by the pseudoreversion of H95N TIM by the S96P mutation. These experiments show that the defect in the H95N mutant isomerase lies in its inability to bind substrate in the planar, *cis* conformation and that this defect is corrected by the S96P pseudoreversion.

## MATERIALS AND METHODS

**Reagents.** DL-Glyceraldehyde 3-phosphate diethyl acetal, glucuronolactone, histidine, streptomycin, ampicillin, reduced nicotinamide adenine dinucleotide (NADH), ethylenediaminetetraacetic acid (EDTA) disodium salt, Dowex-50W ( $\text{H}^+$  form), and QAE Sephadex A-120 were obtained from Sigma Chemical Co. (St. Louis, MO). Poly(ethylene glycol) 8000 was obtained from US Biochemicals (Cleveland, OH). DL-Glyceraldehyde 3-phosphate diethyl acetal was deprotected to DL-glyceraldehyde 3-phosphate according to the manufacturer's instructions, but using 1/10th the volume of  $\text{H}_2\text{O}$  so that the resulting solution was 10 times as concentrated. Phosphoglycolohydroxamate was prepared by J. Belasco. Bromohydroxyacetone phosphate (BHAP) was prepared as described by de la Mare et al. (1972). Glycerol-3-phosphate dehydrogenase was obtained from Boehringer-Mannheim and was made free of TIM activity by centricron ultrafiltration of a 1 mL sample of the protein against 100 mM triethanolamine-hydrochloride, pH 7.6, 1 mM EDTA. The dialyzed protein was then treated with a 100-fold molar excess of BHAP for 1 h on ice and "Centriconed" with three buffer changes to remove the excess BHAP. Oligonucleotides were prepared on a Milligen 7500 DNA synthesizer according to the manufacturer's protocols and were not further purified before use. All other reagents were from commercial sources and were used without further purification. Specifically  $^{13}\text{C}$ -labeled substrates used in the FTIR experiments were prepared as described in Komives et al. (1991).

**Protein Production.** The gene for each mutant was prepared by mutagenesis of the gene for wild-type TIM from chicken muscle contained in a phagemid vector that was a derivative of pBS+/- and has been described (Blacklow & Knowles, 1990). This phagemid vector allowed the efficient production of single stranded DNA for mutagenesis. The phagemid contains, on an *EcoRI* to *PstI* fragment, the *trc* promoter upstream from the complete TIM gene and allowed the production of 50–80 mg of protein per liter of cells. The expression vectors were used to transform *E. coli* strain DF502, which is a strep<sup>R</sup>, tpi<sup>-</sup> strain that was kindly provided by D. Fraenkel and has been previously described (Straus & Gilbert, 1985).

Large amounts of pure protein were prepared by growing the bacterial transformants in a final volume of 10 L of M63 salts (Miller, 1972) containing casamino acids (0.5% w/v), glucuronolactone (0.4% w/v), glycerol (0.1% w/v),  $\text{MgSO}_4$  (1 mM), thiamine (1 mg/mL), L-histidine (80 mg/L), strep-

tomycin (100 mg/L), and ampicillin (200 mg/L). Cells were harvested after 12–20 h by centrifugation at 3000g. The cells were lysed in a continuous-flow French pressure cell (Aminco, Urbana, IL), and the lysate was centrifuged at 8500g for 1 h to remove cell debris. The ammonium sulfate fraction from 55% to 90% saturation was collected and dialyzed against TE buffer (10 mM Tris-HCl, pH 7.8, 1 mM EDTA) overnight. The following day, the crude protein was loaded onto a 300 mL column of QAE Sephadex A-120 equilibrated with TE buffer, and eluted with a linear gradient of 0–300 mM KCl (1 L to 1 L). The proteins were finally purified on a MonoQ 10/10 column using the same gradient. Purity of the proteins was assessed by silver staining overloaded 15% SDS–PAGE gels (Laemmli, 1970). Concentration of the protein was afforded by Centriprep and Centricon concentration (Amicon, Danvers, MA). The purified protein was assayed for conversion of glyceraldehyde 3-phosphate to dihydroxyacetone phosphate according to the method of Blacklow and Knowles (1990), and the  $k_{\text{cat}}$  and  $K_m$  values obtained were identical to those previously reported.

**Protein Crystallization.** The purified protein was dialyzed into MilliQ H<sub>2</sub>O and concentrated to 20 mg/mL (calculated by taking the absorbance at 280 nm and multiplying by the extinction coefficient of chicken TIM of 1.21 mg/OD). A 0.5 M solution of phosphoglycolohydroxamate (PGH) in water was prepared by mixing 2 mg of PGH in 25  $\mu$ L of MilliQ H<sub>2</sub>O. For 1.5 mM final concentration of PGH in the crystallization drop, 115.2  $\mu$ L of protein was mixed with 4.8  $\mu$ L of PGH solution. Initially, crystallization conditions were screened using vapor diffusion of hanging drops by the method of Jancarik and Kim (1991). Crystals appeared at room temperature after 4–7 days in the well containing 100 mM Tris buffer, pH 8.5, 200 mM lithium sulfate, and PEG 8000. We found that crystals appeared at a wide range of PEG 8000 concentrations, and we routinely set up several wells containing concentrations of PEG 8000 from 12.5% to 21% in 2.5% increments. Several crystals were obtained from this range of PEG concentrations, but the exact concentration of PEG 8000 was not reproducible. The crystals grow as elongated prisms and belong to the space group  $P2_12_12_1$ , with one dimer per asymmetric unit and cell dimensions of  $a = 136.26$ ,  $b = 74.06$ ,  $c = 57.30$  for the H95N single mutant and  $a = 136.04$ ,  $b = 74.09$ ,  $c = 57.33$  for the H95N·S96P double mutant. The crystals were mounted in quartz capillary tubes with mother liquor containing PGH on either side to prevent the crystal from drying out.

**X-ray Crystallographic Data Collection and Processing.** For each of the single and double mutant isomerases, a high-resolution data set was collected on the San Diego Mark II Multiwire area detector system with two multiwire proportional chambers (Cork et al., 1973; Xuong et al., 1985a,b). The H95N single mutant crystal diffracted to better than 1.95 Å resolution. To assure completeness, the whole data set was collected from a total of nine orientations based on the data collection strategy of Hamlin et al. (1985) and contained 39 362 unique reflections out of 114 538 observed reflections (Table 2). The H95N·S96P double mutant crystal diffracted to better than 1.94 Å resolution. The data set contained 96 078 reflections measured, out of which 36 521 were unique reflections, collected from ten orientations of the crystal. Both data sets were processed using the UCSD data

Table 2: Statistics of Data Collection and Refinement for the H95N and H95N·S96P Mutant Isomerase Structures

	H95N TIM	H95ND·S96P TIM
data collection		
unit cell parameters	$a = 136.3$ Å	$a = 136.1$ Å
	$b = 74.1$ Å	$b = 74.1$ Å
	$c = 57.3$ Å	$c = 57.3$ Å
space group	$P2_12_12_1$	$P2_12_12_1$
resolution range	13.0–1.95 Å	12.0–1.94 Å
no. of total reflections	114 538	96 078
no. of unique reflections	39 362	36 521
$R_{\text{sym}}$ (on I) <sup>a</sup>	7.7%	6.7%
data completeness	92%	85%
refinement		
resolution range	6.0–1.95 Å	6.0–1.94 Å
$R$ -factor <sup>b</sup>	17.6%	18.3%
no. of reflections ( $I/\sigma(I) > 0$ )	37 990	35 189
no. of protein atoms	3708	3710
no. of inhibitor atoms	20	20
no. of water molecules	286	349
deviation from ideal geometry (rmsd)		
bond distances	0.014 Å	0.014 Å
angle distances	2.6°	2.6°
planar distances	0.014 Å	0.014 Å

<sup>a</sup>  $R_{\text{sym}} = \sum (|I(h,j) - I(h)|) / \sum I(h,j)$ , where  $I(h,j)$  are symmetry-related intensity observations and  $I(h)$  is the mean intensity of reflections with unique indices  $h$ . <sup>b</sup>  $R$ -factor =  $\sum ||F_o| - |F_c|| / \sum |F_o|$ .

reduction package giving completenesses of 92% and 85%, respectively (Table 2).

**Structure Determination.** Since both the single and double mutant isomerase crystals were isomorphous with those of wild-type TIM complexed to PGH (Zhang et al., 1994), the mutant structures were solved by simple difference Fourier methods.

Refinement of the two crystal structures was carried out using X-PLOR (Brunger, 1988). Interleaved between refinement sessions were model rebuilding sessions on an Evans & Sutherland PS330 graphics system using the modeling program FRODO (Jones, 1978; Sack, 1988). The procedure for both mutant structure refinements was exactly the same. Phases were calculated from the wild-type chicken TIM-PGH (Zhang et al., 1994) model coordinates with the PGH active site residues (N11, K13, H95, S96, and E165) and flexible loop residues (166–176) deleted. A difference Fourier electron density map with coefficients ( $3F_o - 2F_c$ ) was calculated using all data from 10.0 to 2.5 Å. The map showed clear electron density over the whole of the dimer model including well-defined densities for the active site residues omitted from the model, and the flexible loop residues in the “closed” position.

Manual modifications to the model were made to introduce two PGH molecules into the active sites of the two subunits, to build in the two 11-residue “lid” loops which close over the active site upon PGH binding, and to add the side chains for residues N11, K13, H95, and S96. For the H95N mutant isomerase, density for the E165 side chain as well as for the PGH molecule were not well defined after the first round of refinement, and for the H95N·S96P double mutant, the density for PGH was not well defined. Therefore, for both mutant isomerases, a second round of X-PLOR refinement was carried out with all the reflection data up to 1.95 Å before building in these residues. After slow cooling

refinement starting at 4000 °C and allowing group and individual *B*-factor refinements, clear density was observed for the E165 side chain and for the PGH molecule. Two final rounds of X-PLOR refinement were carried out to improve the final quality of the map.

The final stage of refinement involved picking water molecules. A difference Fourier map with coefficients ( $F_o - F_c$ ) was calculated and the potential water candidates were picked based on peaks at the  $3\sigma$  level and higher with reasonable hydrogen bonding partners. A checking procedure after refinement eliminated those candidates with *B*-factors higher than 50.0 Å<sup>2</sup>. The final model of each mutant TIM complexed with PGH was refined against all of the merged area detector data between 6.0 and 1.95 Å resolution using all reflections with  $I/\sigma(I) > 1$ . The final *R*-factors of the H95N and H95N•S96P mutant TIM-PGH structures were 17.6% and 18.3%, respectively (Table 2).

**FTIR Spectroscopy.** Infrared absorbance spectra were recorded using an FTS-40 instrument (Digilab, Cambridge, MA) equipped with a temperature-controlled micro Circle cell (Spectra-Tech, Stamford, CT). The sample compartment was purged with dry N<sub>2</sub> for several hours after installation of the Circle cell and before injection of the protein samples, to minimize water vapor absorbances in the spectra. The spectral resolution was 2 cm<sup>-1</sup> and the number of scans accumulated per Fourier transform was 1024. The time required for data acquisition was 20 min. The samples were cooled to 8 °C. The protein samples were first concentrated to 200–300 mg/mL and then exchanged into deuterated buffer that had been prepared by lyophilizing 100 mM Tris-HCl buffer, pH 7.6, containing EDTA (1 mM) and then dissolving this residue in D<sub>2</sub>O. The buffer had a pD of approximately 8. The volume of sample required to fill the Circle cell and connecting tubing was approximately 60 μL. The Circle cell was exhaustively washed with buffer between each filling with sample and cleaned daily with a dilute solution of low-foaming detergent, and finally washed extensively with H<sub>2</sub>O. Protein (70 μL, 10 mN final concentration of active sites) was mixed with substrate (4 μL, 14 mM final concentration) immediately before the sample was injected into the Circle cell.

To obtain spectra of enzyme-bound species, appropriate subtractions of the spectra of free substrate and of free enzyme were made. These subtractions have a negligible effect on the region of the spectrum from 1700 to 1760 cm<sup>-1</sup> but reduce the absorbance below 1700 cm<sup>-1</sup>.

## RESULTS

**Position of Active Site Residues in the H95N and H95N•S96P Mutant TIMs.** Both the H95N single mutant and the H95N•S96P double mutant have an overall structure that is unchanged from that of the wild-type chicken enzyme. Most of the side chains in the active site do not move in the single mutant when H95 is changed to asparagine (Figure 2A,B). In particular, K13, E97, and the flexible loop (residues 166–176) are positioned identically as in the wild-type structure. The Nδ of N95 in both the single and double mutants is located in the same place as the Nδ of H95 in the wild-type enzyme.

Glutamate 165 has different positions in the loop-closed, PGH complex and in the loop-open substrate-free form of the wild-type enzyme. In the PGH complex, Oε2 of E165

Table 3: Distances (in Å) between Atoms within the Active Sites of the H95N and H95N•S96P Mutant Isomerases Compared to Those of the Wild-Type Isomerase

	H95N TIM		H95N•S96P TIM		wild-type TIM	
Oε2 of E165 to C1 of PGH <sup>a</sup>	4.1 <sup>b</sup>	4.3	3.2	3.5	2.6	2.6
Oε2 of E165 to N2 of PGH	3.5	3.3	4.1	3.8	3.4	3.4
Oε2 of E165 to O1 of PGH	4.4	3.5	3.4	3.4	2.9	2.9
Oε2 of E165 to O2 of PGH	2.6	2.8	3.2	3.2	4.3	4.3
Nε of H95 to O1 of PGH	N/A		N/A		2.9	2.9
Nδ of N95 to O1 of PGH	4.9	4.6	4.1	3.7	N/A	
Nε of H95 to O2 of PGH	N/A		N/A		2.8	2.8
Nδ of N95 to O2 of PGH	6.0	6.0	4.0	4.0	N/A	
Nζ of lysine 13 to O2 of PGH	5.6	5.6	3.9	4.2	2.6	2.6
H <sub>2</sub> O 683/761 <sup>c</sup> to O1 of PGH	2.8	3.2	not present		not present	
H <sub>2</sub> O 683/761 to O2 of PGH	3.7	3.6	not present		not present	
H <sub>2</sub> O 683/761 to Oε2 of E165	3.4	3.4	not present		not present	
H <sub>2</sub> O 683/761 to Nδ of N95	3.4	3.4	not present		not present	
H <sub>2</sub> O 683/761 to H <sub>2</sub> O 772/712 <sup>d</sup>	3.2	3.5	not present		not present	
H <sub>2</sub> O 772/712 to O1 of PGH	3.2	2.5	not present		not present	
H <sub>2</sub> O 772/712 to O2 of PGH	4.2	4.5	not present		not present	
H <sub>2</sub> O 772/712 to Oε2 of E165	3.2	3.1	not present		not present	
H <sub>2</sub> O 772/712 to Nδ of N95	2.8	2.6	not present		not present	
H <sub>2</sub> O 772/712 to Oγ of S96	3.0	2.7	not present		not present	
H <sub>2</sub> O 607 to O1 of PGH	N/A	4.2	N/A		N/A	
H <sub>2</sub> O 607 to O2 of PGH	N/A	2.9	N/A		N/A	
H <sub>2</sub> O 607 to Oε2 of E165	N/A	3.3	N/A		N/A	
H <sub>2</sub> O 607 to Oε1 of E165	N/A	2.7	N/A		N/A	
H <sub>2</sub> O 607 to Nδ of N95	N/A	2.8	N/A		N/A	

<sup>a</sup> The reported distance is to Oε1 of E165 for the wild-type isomerase.

<sup>b</sup> The first number corresponds to the distance measured in subunit A of the dimeric isomerase, and the second number corresponds to the distance measured in subunit B. <sup>c</sup> Water 683 is in subunit A, and water 761 is in subunit B of the H95N mutant isomerase. <sup>d</sup> Water 772 is in subunit A, and water 712 is in subunit B of the H95N mutant isomerase.

forms the apex of a square pyramid, the base of which is formed by the enediol plane represented in the substrate analog by O2-N2-C1-O1 (Figure 2). In the substrate-free form, the side chain of E165 is tilted away from the substrate and is within hydrogen-bonding distance of the hydroxyl group of S96 (Figure 3). Due to its different interactions with E165, in the substrate-free form of the wild-type enzyme, S96 is hydrogen bonded to Oε2 of E165. Upon PGH binding, the hydrogen bond between E165 and S96 is broken, and the side chain of S96 rotates to hydrogen bond to a network of water molecules. In both the single H95N and in the double H95N•S96P mutant enzymes, the side chain of E165 is tilted away from its wild-type position toward the position it has in the unliganded enzyme. In the single mutant, H95N, structure, the carboxylate group is displaced some 2.5 Å from its position in the loop-closed structure of the wild-type enzyme (Table 3). It is difficult to explain why the mutation of H95 to N would cause the side chain of E165 to be displaced so dramatically, but it appears to have resulted from a combination of the displacement of O2 of the PGH molecule as well as of S96. A similar tilt was observed for this residue in the yeast H95Q structure (Komives et al., 1991). In the H95N mutant, the Oγ of S96 is 3.1 Å away from Oε2 of E165. Thus, the side chains of both E165 and S96 are in similar positions in the PGH-bound form of the H95N mutant isomerase as in the substrate-free form of the wild-type isomerase (Figure 3).

The structure of the active site of the H95N•S96P double mutant is more like the PGH-bound wild-type enzyme than the substrate-free form. The E165 side chain has moved back toward the position it has in the PGH-bound form of

the wild-type enzyme from its position in the H95N single mutant (Figure 2C,A). The position of the carboxyl group of E165 has partially but not completely recovered the position it had in the wild-type PGH complex, and O $\epsilon$ 2 is still 1.2 Å away from its position in the wild-type enzyme. Movement of the PGH closer to the E165 partly compensates for the alteration in position of the carboxyl group of E165 such that the distance between O $\epsilon$ 2 and the protons of the substrate is less than 1 Å longer than in the wild-type structure. Introduction of the bulkier proline side chain in the active site pocket has no effect on the backbone conformation because the  $\phi$ -angle of S96 in the wild-type structure is already optimal for a proline. The introduction of the proline side chain in place of the serine appears to alter the number of observed ordered water molecules in the active site so that only one water molecule is observed near the E165 side chain, whereas two are observed in the wild-type and H95N mutant isomerase structures (Zhang et al., 1995). Also, only one water molecule is observed between the substrate and the N $\delta$  of N95 in the H95N·S96P double mutant whereas two were observed in the H95N single mutant isomerase (Figure 2A,C).

*Changes in the Conformation and Position of the Intermediate Analog.* The conformation of the PGH intermediate analog may represent the conformation of bound substrate. Figure 4 shows the various configurations of the PGH molecule in the different mutant isomerases and in the different subunits of these isomerases. The conformation of the PGH molecule is radically altered in the H95N single mutant isomerase. Whereas the dihedral angle formed by the O2-N2-C1-O1 atoms of the PGH is 4°, or almost 0° in the wild-type isomerase, this angle in the H95N mutant isomerase is 113° in the A subunit and 66° in the B subunit, or approximately 90° off of planarity. The electron density of the PGH could not be fit to a single conformation of PGH. The structures were solved using averaging of the two subunits, so it is not clear whether this is due to two conformations of PGH, that have similar energies each in some subunits, or to conformational averaging of PGH molecules within the same subunit. For purposes of clarity, we have modeled one conformation in the active site of subunit A, and the other conformation in the active site of subunit B in the crystal structure. Both conformers show a radically altered position of O2 of PGH compared to its position in the wild-type PGH complex (Figure 4). Because of the nonplanar conformation of the O2-N2-C1-O1 atoms of the PGH, the O2 of PGH is angled upward so that it is very close to O $\epsilon$ 2 of E165, 2.6–2.8 Å away. This distance is even closer than the 2.9 Å observed in the wild-type enzyme. A comparison of the two conformers of PGH shows that the position of O2 is similar, while the position of O1 is different. Thus, O2, which is out of plane compared to the wild-type conformation, is 6 Å away from the N $\delta$  of H95 in both conformations. Although O1 occupies a similar position to O1 in the wild-type PGH complex, its position differs slightly between the two different conformers of PGH observed in the H95N mutant isomerase. Thus, O1 is 4.9 Å away from the N $\delta$  of H95 in one conformer and 4.6 Å away in the other conformer. Distances of O1 to the O $\epsilon$ 2 of E165 are also different for the two conformers, as are distances to the H<sub>2</sub>O(772/712), which appears to take the place of H95 in the H95N structure. In fact, the distance of O1 to H<sub>2</sub>O(772/712) is 3.2 Å in one conformer (modeled in

subunit A) and 2.5 Å away in the other (modeled in subunit B). This is interesting because it seems to correlate with the observation of two carbonyl stretching frequencies for the DHAP carbonyl (which should occupy the same site as O1 of PGH). One might hypothesize that just as for the PGH substrate analog bound at the active site of the crystalline TIM is apparently in two conformations, DHAP bound at the active site of the highly concentrated TIM in the IR sample may be also in two conformations.

The conformation of the PGH in the H95N·S96P double mutant isomerase closely resembles the conformation in the wild-type TIM-PGH complex. The PGH O2-N2-C1-O1 dihedral angle is 10° in the subunit A structure and 7° in the subunit B structure, so that it is again close to 0° and close to the wild-type structure. When the backbones of the isomerase subunits for the different mutants are superimposed, all of the phosphate groups are, within error, superimposed. There is a slight displacement of the PGH inhibitor in the H95N·S96P double mutant isomerase compared to the wild-type isomerase, the N of the PGH appears to be lower in the active site by 0.9–1.0 Å than in the wild-type. The O2 follows this difference, but the C1 and O1 positions superimpose well on the positions of these atoms in the wild-type structure (Figure 4). Thus, the PGH appears to be somewhat twisted in its location in the active site of the H95N·S96P double mutant isomerase. This difference results in an increase of 0.6–0.9 Å in the distance from the N of PGH to O $\epsilon$ 2 of E165 from 2.6 Å in the wild type to 3.2–3.5 Å in the H95N·S96P double mutant. The distance from the C1 of PGH to O $\epsilon$ 2 of E165 is also 0.4–0.7 Å longer, increasing from 2.9 Å to 3.8–4.1 Å.

*Substrate Carbonyl Polarization.* It had been observed previously that the carbonyl group of DHAP, which has an infrared absorbance of 1730 cm<sup>-1</sup> in solution is shifted to lower wavenumbers when DHAP is bound at the active site of wild-type TIM (Belasco & Knowles, 1980). The hypothesis that H95 polarizes the carbonyl group of DHAP was shown to hold when mutation of H95 to N resulted in substrate carbonyl stretching frequencies of 1742 cm<sup>-1</sup>, and therefore complete loss of substrate polarization by the enzyme (Komives et al., 1991). The FTIR spectra of an equilibrium mixture of DHAP and GAP bound to the H95N single mutant isomerase and the H95N·S96P double mutant isomerase are shown in Figure 5A and B. The identity of the observed absorbance bands were determined by selective <sup>13</sup>C labeling, and the spectra observed for the equilibrium mixture of 1-<sup>13</sup>C substrates and U-<sup>13</sup>C substrates are also shown. In each case, the starting labeled substrate was allowed to equilibrate on the enzyme surface, so the amount of observed carbonyl for each of DHAP and GAP is related to the internal equilibrium constant for bound GAP versus bound DHAP. Starting with [1-<sup>13</sup>C]GAP produces both [1-<sup>13</sup>C]DHAP, for which the carbonyl is still visible, and [1-<sup>13</sup>C]GAP for which the carbonyl stretching frequency drops by some 40 cm<sup>-1</sup> into the region below 1700 cm<sup>-1</sup> in which the peptidyl amide carbonyl resonances obscure its observance. The absorption bands for each carbonyl stretch can therefore be identified according to when they disappear (Komives et al., 1991, 1995).

For the H95N single mutant isomerase, two bands are observed that can be assigned to the carbonyl group of DHAP, at 1723 and 1732 cm<sup>-1</sup> (Figure 5A). In the crystal structure, the O1 of PGH (which replaces the carbonyl group



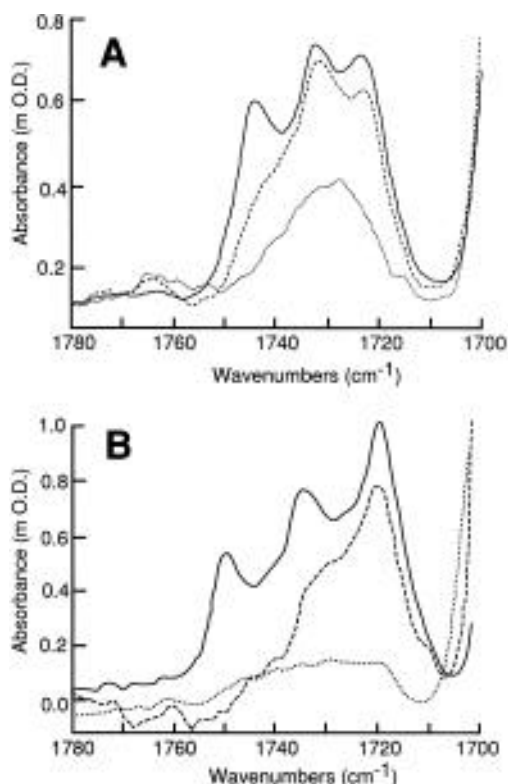


FIGURE 5: A. Fourier transform infrared spectrum of substrates bound to the single mutant H95N isomerase. The spectrum of unlabeled substrates bound to the isomerase (solid line) shows bands at 1723, 1732, and 1745 cm<sup>-1</sup>. Labeling of the substrates with <sup>13</sup>C in the 1-position (dashed line) shows the loss of the GAP carbonyl stretch which can therefore be assigned to the 1745 cm<sup>-1</sup> band. Labeling of the substrates with <sup>13</sup>C at all positions (dotted line) causes the loss of both remaining bands which can therefore be assigned to DHAP. B. Fourier transform infrared spectrum of substrates bound to the double mutant H95N-S96P isomerase. The spectrum of unlabeled substrates bound to the isomerase (solid line) shows bands at 1717, 1734, and 1748 cm<sup>-1</sup>. Labeling of the substrates with <sup>13</sup>C in the 1-position (dashed line) shows the loss of two bands which can be assigned to GAP carbonyl stretches at 1734 and 1748 cm<sup>-1</sup>. Labeling of the substrates with <sup>13</sup>C at all positions (dotted line) causes the loss of the band at 1717 cm<sup>-1</sup> which can therefore be assigned to DHAP.

of DHAP) is also in two different locations 3.2 Å (in subunit A) or 2.5 Å (in subunit B) away from the H<sub>2</sub>O(772/712) that bridges between the substrate analog and Nδ of N95. On the other hand, O2 of PGH (which replaces the GAP carbonyl) is in the same location in both subunits, and the GAP carbonyl shows a single stretching frequency of 1745 cm<sup>-1</sup>. Comparing this result with that obtained for the H95Q mutant, it seems that the GAP carbonyl is not polarized at all by the enzyme, and this is consistent with it occupying the same site occupied by O2 of PGH, which is quite distant from N95 and from H<sub>2</sub>O(772/712). In the H95Q mutant, the carbonyl group of DHAP was also not polarized by the mutant enzyme (Komives et al., 1991). The observation of two carbonyl stretching bands for DHAP in the H95N mutant suggests that at least some of the time, the DHAP carbonyl is more polarized than it was in the H95Q mutant, and this is probably due to the presence of H<sub>2</sub>O(772/712) (see below).

The absorbance bands corresponding to the carbonyl stretching frequencies of the DHAP and GAP in the double mutant isomerase also can be rationalized by the structure. In this case, two bands were observed for the GAP carbonyl at 1734 and 1748 cm<sup>-1</sup> and a single band was observed for

the DHAP carbonyl at 1717 cm<sup>-1</sup> (Figure 5B). The rationale in this case relates to the presence of a single H<sub>2</sub>O(607) which is only present in one subunit of the isomerase, and which had a particularly high *B* factor (59.4). This water molecule is within hydrogen bonding distance to both carbonyls of E165 and to O2 of PGH, which corresponds to the GAP carbonyl. H<sub>2</sub>O(607) is highly disordered, and whether or not it is present and/or hydrogen bonded to the GAP carbonyl may explain the observation of two carbonyl stretches for this group.

**Changes in Positions of Bound Water Molecules.** In the wild-type isomerase, two ordered H<sub>2</sub>O molecules are observed near the side chain of E165 (356/390 and 360/399). These two water molecules were no longer observed when the S96P mutation was introduced at the active site, presumably because this mutation alters the hydrophobicity of the active site. In the single mutant H95N mutant isomerase, two water molecules are again observed near E165 (772/712 and 677/375), but their positions relative to the carboxylate oxygens are very different from those observed for the wild-type isomerase. In addition, one new water molecule is observed, H<sub>2</sub>O(683/761), which bridges the Nδ of N95 and the substrate analog oxygen atoms. No water molecules are observed near the substrate analog in the wild-type isomerase structure (Zhang et al., 1995). The water molecules near the substrate analog (772/712 and 683/761) are observed in both subunits of the H95N mutant isomerase, and they are within hydrogen-bonding distance of E165, N95, and PGH. In fact, H<sub>2</sub>O(683/761) is 2.8/3.2 Å away from O1 of PGH, 3.7/2.5 Å away from O2 of PGH, and 3.4 Å away from Oε2 of E165. H<sub>2</sub>O(772/712) is 3.2/2.5 Å away from O1 of PGH, 4.2/4.5 Å away from O2 of PGH, 3.2/3.1 Å away from Oε2 of E165, and 2.8/2.6 Å away from Nδ of N95. The two waters are also within hydrogen-bonding distance of each other (3.2/3.5 Å).

As was observed for the E165D-S96P double mutant isomerase, the S96P mutation appears to reduce the number of ordered water molecules in the active site of the isomerases. Only a single water molecule is present near the E165 side chain in the H95N-S96P structure, H<sub>2</sub>O(728/853). In one subunit of the dimer of the H95N-S96P double mutant, a highly disordered water molecule with a *B* factor of 59.4, is present. This water molecule, H<sub>2</sub>O(607) is 2.9 Å away from O2 of PGH, and 2.8 Å away from Nδ of N95. It is also not far from O1 of PGH (4.2 Å), from Oε2 of E165 (3.3 Å) and from Oε1 of E165 (2.7 Å). The fact that this enzyme was found to follow the wild-type mechanism for proton transfers strongly suggests that there is indeed a water molecule present in this position that can transfer protons to and from the substrate oxygens during the catalytic reaction (Blacklow & Knowles, 1990).

## DISCUSSION

**Structural Consequences of the H95N Mutation.** When histidine 95 is changed to asparagine, the catalytic efficiency of the chicken isomerase is reduced 3000-fold. The complete kinetic analysis of this mutant showed that the catalytic steps were rate limiting, and that substrate binding was unaffected, but damage to *k*<sub>cat</sub> accounted for all of the rate reduction (Table 1). The mutation was designed to assess the importance of substrate carbonyl polarization in the triosephosphate isomerase reaction, but without structural information it was

impossible to determine whether other detrimental affects were also introduced. Indeed, the structure presented here shows that the mutation of H95 to N alters the conformation of PGH. It is no longer in the coplanar, *cis* conformation, and O2, which is ordinarily interacting with the N $\epsilon$  of H95, is now angled upward to interact with O $\epsilon$ 2 of E165. Just as Daggett and Kollman (1990) predicted from molecular dynamics calculations, mutation of H95 to N results in distortion of the O2-N2-C1-O1 plane of PGH, and of the substrate. It is difficult to imagine how the catalytic reaction proceeds from such a nonplanar conformation, and this may explain why the  $k_{\text{cat}}$  is so low for this isomerase mutant. The observation of a nonplanar conformation of the PGH substrate analog in the H95N mutant isomerase structure also helps to explain the fact that this mutant isomerase produces three methylglyoxal molecules for every 10 turnovers to either DHAP or GAP. This ratio is not as poor as the mutant in which the phosphate-binding loop was deleted, which produced three methylglyoxal molecules for every single turnover to either DHAP or GAP (Pompliano et al., 1990). If stereoelectronic arguments hold, the rate of methylglyoxal production is expected to be rapid whenever orbital overlap can occur between the DHAP carbonyl group and the phosphate ester bond. Removal of the phosphate binding loop would therefore be expected to cause the elimination reaction more readily than mutation of a catalytic residue. In fact, the phosphate group of the substrate analog is in exactly the same location in the H95N mutant as it is in the wild-type isomerase. If the catalytic mechanism is slow enough, however, one might expect some production of methylglyoxal even if orbital overlap is not optimal. The observed conformation for the PGH analog is definitely not optimal for proton abstraction, and this suggests that slow reprotonation of the enediolate could be the cause of methylglyoxal production in this mutant.

*Why the H95N·S96P Pseudorevertant is Improved.* The S96P second site alteration was found to improve both the E165D and the H95N catalytic lesions in triosephosphate isomerase. The mechanism by which it repairs the E165D mutation apparently involves stabilization of the first intermediate in the reaction (Komives et al., 1995). The mechanism by which it repairs the H95N lesion apparently involves restoration of the conformations of E165 and PGH from their altered positions in the H95N single mutant isomerase toward the conformations they have in the wild-type PGH—*isomerase* complex. Indeed, the PGH conformation in the H95N·S96P pseudorevertant structure is again coplanar *cis*, and very similar to that seen in the wild-type isomerase. If the nonplanar conformation of the PGH in the H95N mutant complex reflects an altered conformation of the substrate, as the FTIR data would suggest, then the return of the substrate to its normal conformation may result in better catalysis. It is also possible that secondarily the  $pK_a$  of the E165 catalytic base is increased by the absence of the water molecules that create a hydrogen bonding environment near the carboxylate. This affect was also suggested for the E165D·S96P pseudorevertant. It is interesting that the S96P mutation does not affect the dramatically longer distance between O $\epsilon$ 2 of E165, the catalytic base, and the substrate protons that would be abstracted in the reaction (Table 3). This was also true in the case of the E165D and E165D·S96P mutant isomerases, and it is possible that the longer distance from O $\epsilon$ 2 of E165 to the protons it must

abstract is compensated for by the increase in  $pK_a$  from the increased hydrophobicity of the environment around E165 due to the proline substitution.

*Water Molecules Take Over Role of H95.* The alteration of H95 to glutamine in the yeast isomerase resulted in a mutant isomerase that followed a completely different mechanism of proton transfers in which E165 apparently transferred protons to and from the substrate oxygens in lieu of the mutated histidine (Nickbarg et al., 1988). Tritium transfer experiments showed that the H95N mutant did not follow the H95Q mechanism. This led to the hypothesis that perhaps a water molecule could fit into the active site when histidine was replaced by asparagine and not when it was replaced by glutamine, and that this water molecule could carry out the proton transfers ordinarily done by the histidine. Proof of this hypothesis has been obtained by the structures presented here, which show clearly the presence of water molecules that apparently bridge the asparagine side chain and the substrate analog oxygen atoms. The observation of these catalytically important water molecules is also consistent with the observation that the substrate carbonyls are polarized to a greater degree in the H95N and H95N·S96P isomerases than in the H95Q mutant isomerase (Table 1).

A single water molecule is apparently responsible for proton transfers in the catalytically more efficient H95N·S96P mutant, while two are present in the H95N single mutant. It is not obvious why one water molecule would be better than two, and for each structure, the distances between the water molecules and the substrate analog oxygens are not so close as to constitute an unusually strong hydrogen bond. These water molecules appear to be responsible for polarizing the substrate carbonyls (see below) and for carrying out the proton transfers ordinarily carried out by H95. The difference in their number and their positions, however, cannot explain the improved catalytic potency of the H95N·S96P pseudorevertant.

*Polarization of the Substrate Carbonyls in the Mutant Isomerases.* The FTIR data could not be interpreted without structural information. The observation of two absorbance bands for DHAP in the H95N mutant, and two bands for GAP in the pseudorevertant complicated the issue further. Although the assumption was always made that the conformation of the substrate analog, PGH, in the crystal structures was a good representation of the conformation of the substrate, this assumption could not really be tested. The H95N and H95N·S96P structures provide an opportunity to test this hypothesis, since more than one conformation (or hydration state in the case of the H95N·S96P isomerase) is observed for the PGH and for the carbonyl groups of the substrate by FTIR. Indeed, these two pieces of data confirm one another; in the H95N structure, the O2 of PGH, which corresponds to the GAP carbonyl, is in the same location in both conformations of PGH, and only one carbonyl absorbance band is observed. The O1 of PGH is in two different locations, 3.2 vs 2.5 Å away from an ordered water molecule, and two carbonyl stretching frequencies are observed for the corresponding carbonyl of DHAP. Similar correlations can be drawn for the H95N·S96P isomerase.

It is interesting that the carbonyl stretching frequencies correlate log-linearly with  $k_{\text{cat}}$  (Figure 6). This implies that the more polarized the substrate carbonyl groups are by the enzyme, the higher will be the catalytic rate, although this

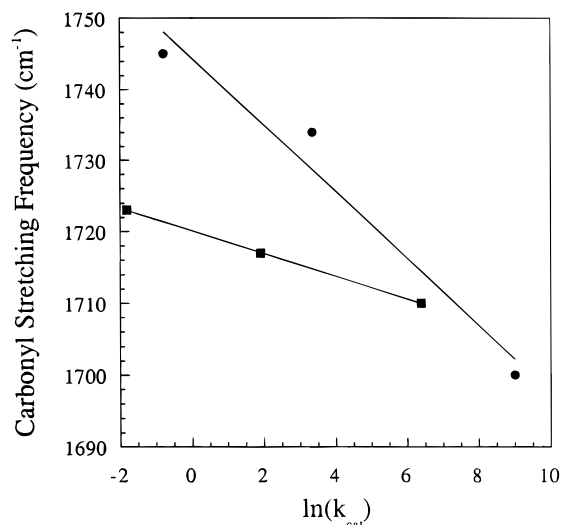


FIGURE 6: Plot of the carbonyl stretching frequencies vs  $\ln(k_{\text{cat}})$  for the single mutant, the double mutant, and the wild-type isomerase. The DHAP carbonyl stretching frequencies (■) are plotted against  $\ln(k_{\text{cat}})$  for the isomerase reaction starting with DHAP, and the GAP carbonyl stretching frequencies (●) are plotted against  $\ln(k_{\text{cat}})$  for the isomerase reaction starting with GAP. For the isomerases which show multiple absorbance bands, only the band at lower wavenumber (more polarized) was used. The wild-type isomerase does not show an absorbance band for GAP, presumably because it is below 1700  $\text{cm}^{-1}$ , so 1700  $\text{cm}^{-1}$  is used as the value for this carbonyl stretching frequency.

is clearly is not the only important factor. The distance between the carboxylate of E165 and the substrate can not, therefore, account for the difference in carbonyl stretching frequencies observed for these two mutant isomerases.

**Conclusion.** Alteration of H95 to N resulted in a mutant triosephosphate isomerase that was not only defective in polarizing the carbonyl groups of the substrate toward the transition state of the reaction, but was also defective at binding the substrate in a single conformation from which catalysis, and not methylglyoxal, formation could occur. The altered conformation of the substrate found in this enzyme not only appeared to make formation of the planar enediolate intermediate difficult, it resulted in a much longer distance between the catalytic base and the substrate protons that would be abstracted in the reaction. Pseudoreversion of the H95N mutant by the S96P second site mutation partially corrected several of the defects from which the H95N mutant suffered. It improved the polarization of both substrate carbonyl groups, and it repositioned the substrate so that it could more easily form the enediolate intermediate. The S96P mutation did not improve the distance between the catalytic base, E165, and the substrate protons that would be abstracted in the reaction.

## ACKNOWLEDGMENT

We thank Jeremy Knowles for inspiring the project and Steven C. Blacklow for many helpful discussions.

## REFERENCES

- Albery, W. J., & Knowles, J. R. (1976) *Biochemistry* 15, 5631–5640.
- Belasco, J. G., & Knowles, J. R. (1980) *Biochemistry* 19, 472–477.
- Blacklow, S. B., & Knowles, J. R. (1990) *Biochemistry* 29, 4099–4108.
- Blacklow, S. C., Raines, R. T., Lim, W. A., Zamore, P. D., & Knowles, J. R. (1988) *Biochemistry* 27, 1158–1167.
- Cork, C., Fehr, D., Hamlin, R., Vernon, W., Xuong, N.-H., & Perez-Mendez, V. (1973) *J. Appl. Crystallogr.* 7, 319–323.
- Daggett, V., & Kollman, P. A. (1990) *Protein Eng.* 3, 677–690.
- Davenport, R. C., Bash, P. A., Seaton, B. A., Karplus, M., Petsko, G. A., & Ringe, D. (1991) *Biochemistry* 30, 5821–5826.
- de la Mare, S., Coulson, A. F. W., Knowles, J. R., Priddle, J. D., & Offord, R. E. (1972) *Biochem. J.* 129, 321–331.
- Deslongchamps, P., Atlani, P., Frehel, D., & Malaval, A. (1972) *Can. J. Chem.* 50, 3405–3408.
- Hamlin, R. (1985) *Methods Enzymol.* 114, 416–52.
- Hermes, J. D., Blacklow, S. C., & Knowles, J. R. (1990) *Proc. Natl. Acad. Sci. U.S.A.* 87, 696–700.
- Jancarik, J., & Kim, S.-H. (1991) *J. Appl. Crystallogr.* 24, 409–411.
- Jones, T. A. (1978) *J. Appl. Crystallogr.* 21, 273–278.
- Kirby, A. J. (1983) *The Anomeric Effect and Related Stereoelectronic Effects at Oxygen*, Springer-Verlag, Berlin.
- Knowles, J. R., & Albery, W. J. (1977) *Acc. Chem. Res.* 10, 105–111.
- Komives, E. A., Chang, L. C., Lolis, E., Tilton, R. F., Petsko, G. A., & Knowles, J. R. (1991) *Biochemistry* 30, 3011–3019.
- Komives, E. A., Loughheed, J. C., Liu, K., Sugio, S., Zhang, Z., Petsko, G. A., & Ringe, D. (1995) *Biochemistry* 34, 13612–21.
- Laemmli, U. K. (1970) *Nature* 227, 680–685.
- Lolis, E., Alber, T., Davenport, R. C., Hartman, F. C., & Petsko, G. A. (1990) *Biochemistry* 29, 6609–6618.
- Lolis, E., & Petsko, G. A. (1990) *Biochemistry* 29, 6619–6625.
- Miller, J. H. (1972) *Experiments in Molecular Genetics*, Cold Spring Harbor Laboratory Press, Plainview, NY.
- Nickbarg, E. B., Davenport, R. C., Petsko, G. A., & Knowles, J. R. (1988) *Biochemistry* 27, 5948–5960.
- Pompliano, D. L., Peyman, A., & Knowles, J. R. (1990) *Biochemistry* 29, 3186–3194.
- Richard, J. P. (1984) *J. Am. Chem. Soc.* 106, 4926–4936.
- Sack, J. S. (1988) PS300 FRODO (version 6.6 revision A) *Molecular Graphics Program for the PS300*. HHMI, Baylor College of Medicine, Houston, TX.
- Straus, D., & Gilbert, W. (1985) *Proc. Natl. Acad. Sci. U.S.A.* 82, 2014–2018.
- Xuong, N.-H., Sullivan, D., Nielson, C., & Hamlin, R. (1985a) *Acta Crystallogr. B* 41, 267–269.
- Xuong, N.-H., Nielson, C., Hamlin, R., & Anderson, D. H. (1985b) *J. Appl. Crystallogr.* 18, 342–350.
- Zhang, Z., Sugio, S., Komives, E. A., Liu, K. L., Knowles, J. R., Petsko, G. A., & Ringe, D. (1994) *Biochemistry* 33, 2830–2837.

BI961556V